REPORT DOCUMENTATION PAGE			Form Approved OMB No. 0704-0188

Public reporting burden for this collection of information is estimated to average 1 hour per response, including the time for reviewing instructions, searching existing data sources, gathering and maintaining the data needed, and completing and reviewing this collection of information. Send comments regarding this burden estimate or any other aspect of this collection of information, including suggestions for reducing this burden to Department of Defense, Washington Headquarters Services, Directorate for Information Operations and Reports (0704-0188), 1215 Jefferson Davis Highway, Suite 1204, Arlington, VA 22202-4302. Respondents should be aware that notwithstanding any other provision of law, no person shall be subject to any penalty for failing to comply with a collection of information if it does not display a currently valid OMB control number. **PLEASE DO NOT RETURN YOUR FORM TO THE ABOVE ADDRESS.**

1. REPORT DATE *(DD-MM-YYYY)*	**2. REPORT TYPE**	**3. DATES COVERED** *(From - To)*
31-10-2012	Final Report	01-11-2009 to 31-10-2012

4. TITLE AND SUBTITLE

Study of Large-Scale Wave Structure and Development of Equatorial Plasma Bubbles Using the C/NOFS Satellite

5a. CONTRACT NUMBER
FA9550-10-C-0004

5b. GRANT NUMBER
N/A

5c. PROGRAM ELEMENT NUMBER
N/A

6. AUTHOR(S)

Tsunoda,Roland T

5d. PROJECT NUMBER
N/A

5e. TASK NUMBER
N/A

5f. WORK UNIT NUMBER
N/A

7. PERFORMING ORGANIZATION NAME(S) AND ADDRESS(ES)

SRI International
333 Ravenswood Ave.
Menlo Park, CA 94025

8. PERFORMING ORGANIZATION REPORT

ERD-19241-FR-12-438

9. SPONSORING / MONITORING AGENCY NAME(S) AND ADDRESS(ES)

USAF, AFRL/ AF Office of Scientific Contract No. FA9550-10-C-0004

875 N. Randolph St. Room 3112
Arlington VA 22203

10. SPONSOR/MONITOR'S ACRONYM(S)

11. SPONSOR/MONITOR'S REPORT NUMBER(S)
AFRL-OSR-VA-TR-2012-1243

12. DISTRIBUTION / AVAILABILITY STATEMENT
Distribution Statement A. Approved for public release, distribution is unlimited"

13. SUPPLEMENTARY NOTES
None

14. ABSTRACT

The development of plasma structure in the nighttime equatorial *F* layer, referred to as equatorial spread *F*, is of strategic importance to the Air Force. These irregularities are responsible for intense scintillations, which can disrupt both communications and navigation. If we hope to achieve short-term forecasting, even on a day-to-day basis, we must understand how the scintillation-producing plasma irregularities, called equatorial plasma bubbles (EPBs), develop. To understand EPB generation and distribution, mounting evidence necessitates knowledge about large-scale wave structure (LSWS), which develops in the bottomside of the *F* layer. A primary obstacle to understanding LSWS has been the paucity of available measurements that can be used to characterize LSWS. With the launch of the Communication/Navigation Outage Forecasting System (C/NOFS) satellite, it became possible, for the first time, to determine LSWS characteristics on a routine basis. The objectives of this project were to collect data that describe LSWS, and to analyze those data (together with other supporting data) to expand our understanding of the underlying physical processes that control development of EPBs. This final report presents the highlights of the results from this study and includes a new, working hypothesis for LSWS and EPB development.

15. SUBJECT TERMS
space weather, short-term forecasting, equatorial spread F, equatorial plasma bubbles, large-scale wave structure, seeding, radio-wave scintillations

16. SECURITY CLASSIFICATION OF:			**17. LIMITATION OF ABSTRACT**	**18. NUMBER OF PAGES**	**19a. NAME OF RESPONSIBLE PERSON**
a. REPORT	**b. ABSTRACT**	**c. THIS PAGE**			Tsunoda,Roland T
unclassified	unclassified	unclassified			

Final Technical Report • October 2012

STUDY OF LARGE-SCALE WAVE STRUCTURE AND DEVELOPMENT OF EQUATORIAL PLASMA BUBBLES USING THE C/NOFS SATELLITE

ERD-19241-FR-12-438
SRI Project Number P19241
Contract Number FA9550-10-C-0004

Prepared by

Roland Tsunoda, Principal Scientist
Center for Geospace Studies
Engineering Research & Development Division
Email: roland.tsunoda@sri.com

Prepared for

Defense Technical Information Center/OCA
8725 John J. Kingman Road, Suite 0944
Fort Belvoir, VA 22060-6217
Email: technicalreports@afosr.af.mil

Approved:

John Kelly, Senior Program Director
Center for Geospace Studies
Engineering Research & Development Division

1 INTRODUCTION

The development of plasma structure in the nighttime equatorial *F* layer, referred to as equatorial spread *F* (ESF), is of strategic importance to the Air Force. These irregularities are responsible for intense scintillations that are imposed on radio signals as they traverse these disturbed regions, and scintillations can disrupt both communications and navigation. Because mitigation is not yet a viable option, emphasis must be placed on short-term forecasting, at least on a day-to-day basis, and preferably with lead times that allow effective strategic planning.

From a space-weather perspective, degradation in communications or navigation from scintillation effects can become crucial in populated zones or in regions of strategic importance. In this regard, the scintillation-producing plasma irregularities, called equatorial plasma bubbles (EPBs), are much more important than those associated with plasma structures confined to the bottomside of the equatorial *F* layer. The reason is that an EPB is a three-dimensional structure in the form of a vertically elongated wedge. The wedge is aligned north-south along geomagnetic field (***B***) lines [*Tsunoda*, 1980], is narrow in longitude, but extended in both altitude and latitude [*Tsunoda et al*., 1982], the latter into both hemispheres. For example, an EPB that reaches an altitude of 1200 km or more, above the magnetic dip equator, also extends in latitude up to and beyond the crest of the equatorial ionization anomaly (EIA). Because the EIA can be thought of as a nominal boundary between the equatorial zone and the more-populated, low-latitude region, these EPBs pose a space-weather problem. (Notice that, although each wedge-like region is longitudinally narrow, almost any radio propagation path will likely intercept an EPB because the wedges are usually inclined to the west of vertical in the plane transverse to ***B***.) Hence, we must be concerned with being able to forecast EPB generation, spatial distribution, and longitudinal transport.

To understand EPB generation and distribution, mounting evidence indicates the necessity of understanding the nature of large-scale wave structure (LSWS), which develops in the bottomside of the *F* layer [*Tsunoda and White*, 1981; *Tsunoda*, 2005, 2008, 2009]. Occurrences of EPBs appear to be confined to regions where upwellings in isodensity contours are associated with LSWS [*Tsunoda and White*, 1981; *Singh et al*., 1997]. These occurrences indicate that LSWS is at least a necessary, if not sufficient, condition for the development of EPBs [*Tsunoda*, 2009; *Li et al*., 2012; *Narayanan et al*., 2012].

A primary obstacle to understanding the nature of LSWS has been the paucity of available measurements to characterize LSWS [*Tsunoda*, 2005]. Until recently, only ALTAIR data have provided direct information about LSWS. With the launch of the Communication/Navigation Outage Forecasting System (C/NOFS) satellite [*de La Beaujardiere et al*., 2004], it became possible, for the first time, to determine LSWS characteristics on a routine basis, by determining the total electron content (TEC) as a function of longitude [*Thampi et al*., 2009; *Tsunoda et al*., 2010, 2011]. To do so, only the differential phase between the two radio beacon signals (150, 400 MHz) from C/NOFS has to be determined. By receiving these beacon signals with a cluster of ground-based receivers near the magnetic dip equator, we can determine TEC variations as a function of latitude as well as longitude, and these variations can be interpreted in terms of LSWS. At the same time, the beacon signals allow the measurement of scintillations produced by plasma structure that exists beneath the orbit of C/NOFS, which cannot be detected by in situ probes on board C/NOFS.

Given the paucity of LSWS data and the opportunity to fill this need by recording the beacon transmissions [*Bernhardt and Siefring*, 2006] from the C/NOFS satellite, we submitted a proposal to collect the data from several receiving stations and to analyze the data with the objective of attaining a much higher level of understanding of LSWS and its role in EPB development. This Final Technical Report summarizes the accomplishments and findings that resulted from the three-year research contract that was awarded in response to our proposal. In the following sections, we describe the status of understanding before the start of the project, and we highlight the accomplishments and scientific results that have ensued over the past three years.

2 STATUS OF UNDERSTANDING BEFORE PROJECT COMMENCEMENT

The notion that LSWS may be playing a central role in EPB development originated from incoherent-scatter (IS) measurements made with ALTAIR, a fully steerable radar [*Tsunoda et al*., 1979], on the Kwajalein Atoll, Marshall Islands [*Tsunoda and White*, 1981]. Figure 1 presents two plots of isodensity contours in the *F* region, which were made from IS measurements during east-west scans with ALTAIR. The scan in the upper panel (22 July 1979) contains tilted contours (higher in the east), which are produced by the post-sunset rise (PSSR) of the *F* layer; this scan shows no evidence of LSWS. The scan in the lower panel (24 July 1979) contains both a tilt and a sinusoidal-like variation, which can be interpreted as the presence of LSWS during the PSSR. On 24 July, LSWS grew in amplitude and was followed by the development of an EPB in each of the crests (upwellings). Prior to these findings, upwellings, which occur in the bottomside *F* layer, were thought to be seed perturbations that become EPBs. In other words, both the seed and the EPB that developed were envisioned to occur and develop in the same background conditions. That is, the driver was either a constant eastward electric field or gravity without a zonal neutral wind [e.g., *Scannapieco and Ossakow*, 1976].

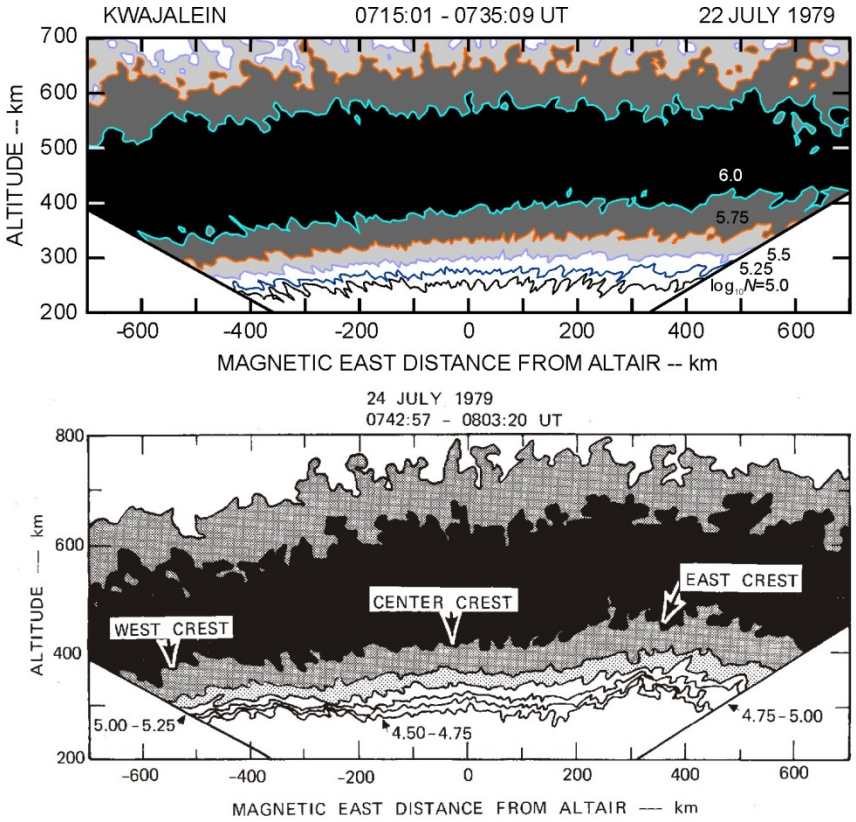

Figure 1. Two maps showing isodensity contours of the *F* layer, which were obtained with ALTAIR during the PSSR. Upper panel: 22 July 1979, when LSWS was not detected. Lower panel: 24 July 1979, when LSWS was detected.

If LSWS is indeed a precursor for EPBs, an understanding of its properties and the underlying physics is the next step toward achieving a space-weather forecasting capability. Some of the key questions that remained to be answered, before the start of this project, included the following:

1. What are the characteristics of LSWS?
2. When does LSWS form?
3. How does LSWS develop?
4. What is the source of LSWS?

The remainder of this report describes and discusses our accomplishments and findings in regard to these key questions.

3 PROJECT ACCOMPLISHMENTS AND FINDINGS

3.1 C/NOFS BEACON DATABASE

A database of measurements of radio beacon transmissions from the C/NOFS satellite has been compiled as part of a joint effort, which included funding support from the National Science Foundation and collaboration with Prof. Mamoru Yamamoto (Kyoto University, Japan). Radio beacon receivers were installed and operated at various field sites during the course of this three-

year effort. Our original intent was to operate three receivers (Pohnpei, Kosrae, and Majuro) for one year, which was then the expected useful lifetime of C/NOFS. This satellite, however, has continued to remain available for scientific studies. Given this rare opportunity to collect more data, we decided to do so for the remainder of the contracting period. This decision allowed us to establish a unique database, which will remain the only one of its kind for the foreseeable future. We have since learned, for example, that the planned, follow-on satellite to C/NOFS will not carry a beacon at 150 MHz. Consequently, TEC measurements made along an equatorial orbit, which are sensitive to small changes in the bottomside *F* layer, will not be possible. We have also learned from various inquiries that opportunities for equatorial launches remain extremely rare.

The research approach for establishing this database has been to perform cluster measurements. That is, by spacing the beacon receivers in both latitude and longitude, we are able to measure variations in TEC that provide two-dimensional (2D) information. As discussed below, 2D information provides clues regarding various questions that have to do with both the seeding and development of EPBs. During the course of the project, we have expanded our original cluster (Pohnpei, Kosrae, and Majuro) in the Pacific sector to include Kwajalein and Guam. The scientific value of the Pacific cluster is enhanced by ionograms being collected with three ionosondes (Kwajalein, Pohnpei, Guam) and a five-beam 50 MHz backscatter radar. During the second year, beacon receivers were installed at Ho Chi Minh City and Nha Trang, which, together with another receiver at Bac Lieu (operated by Prof. Mamoru Yamamoto, Kyoto University), formed a cluster in Vietnam. (Operation of those sites continued for five months.) During the third year, two receivers were installed at Kuala Lumpur and George Town, Malaysia, to extend a larger South-East Asian cluster (operated by Prof. Yamamoto), which spans Thailand, Malaysia, and Indonesia. Data collection is expected to continue in both the Pacific and South-East Asian sectors, throughout the useful lifetime of C/NOFS.

3.2 LIST OF PUBLICATIONS

We have made substantial progress with scientific findings, which directly address the key questions listed above. The results can be found in 16 papers published in peer-reviewed scientific journals. The papers are listed below in chronological order.

Kelley, M.C., F.S. Rodrigues, J.J. Makela, R. Tsunoda, P.A. Roddy, D.E. Hunton, J.M. Retterer, O. de La Beaujardiere, E.R. de Paula, and R.R. Ilma, C/NOFS and radar observations during a convective ionospheric storm event over South America, *Geophys. Res. Lett.*, *36*, L00C07, doi:10.1029/2009GL039378, 2009.

Makela, J.J., M.C. Kelley, and R.T. Tsunoda, First observations of midlatitude ionospheric instabilities generating meter-scale waves at the magnetic equator, *J. Geophys. Res.*, *114*, A01307, doi:10.1029/2007JA012946, 2009.

Thampi, S.V., M. Yamamoto, R.T. Tsunoda, Y. Otsuka, T. Tsugawa, J. Uemoto, and M. Ishii, First observations of large-scale wave structure and equatorial spread *F* using CERTO radio beacon on the C/NOFS satellite, *Geophys. Res. Lett.*, *36*, L18111, doi:10.1029/2009GL039887, 2009.

Tsunoda, R.T., Multi-reflected echoes: Another ionogram signature of large-scale wave structure, *Geophys. Res. Lett.*, 36, L01102, doi:10.1029/2008GL036221, 2009.

Miller, E.S., J.J. Makela, K.M. Groves, M.C. Kelley, and R.T. Tsunoda, Coordinated study of coherent radar backscatter and optical airglow depletions in the Central Pacific, *J. Geophys. Res*., *115*, A06307, doi:10.1029/2009JA014946, 2010.

Tsunoda, R.T., On seeding equatorial spread *F* during solstices, *Geophys. Res. Lett*., *37*, L05102, doi:10.1029/2010GL042576, 2010a.

Tsunoda, R.T., On seeding equatorial spread *F*: Circular gravity waves, *Geophys. Res. Lett*., 37, L10104, doi:10.1029/2010GL043422, 2010b.

Tsunoda, R.T., On equatorial spread *F*: Establishing a seeding hypothesis, *J. Geophys. Res*., *115*, A12303, doi:10.1029/2010JA015564, 2010c.

Tsunoda, R.T., D.M. Bubenik, S.V. Thampi, and M. Yamamoto, On large-scale wave structure and equatorial spread *F* without a post-sunset rise of the *F* layer, *Geophys. Res. Lett*., *37*, L07105, doi:10.1029/2009GL042357, 2010.

Gentile, L.C., W.J. Burke, P.A. Roddy, J.M. Retterer, and R.T. Tsunoda, Climatology of plasma density depletions observed by DMSP in the dawn sector, *J. Geophys. Res*., *116*, A03321, doi:10.1029/2010JA016176, 2011.

Tsunoda, R.T., M. Yamamoto, T. Tsugawa, T.L. Hoang, S. Tulasi Ram, S.V. Thampi, H.D. Chau, and T. Nagatsuma, On seeding, large-scale wave structure, equatorial spread *F*, and scintillations over Vietnam, *Geophys. Res. Lett*., *38*, L20102, doi:10.1029/2011GL049173, 2011.

Thampi, S.V., R. Tsunoda, L. Jose, and T.K. Pant, Ionogram signatures of large-scale wave structure and their relation to equatorial spread *F*, *J. Geophys. Res*., *117*, A08314, doi:10.1029/2012JA017592, 2012.

Tsunoda, R.T., A simple model to relate multi-reflected echoes and satellite traces to large-scale wave structure, *Geophys. Res. Lett*., in press, 2012a.

Tsunoda, R.T., On seeding equatorial spread *F*: Parallel or transverse transport? *J. Atmos. Solar-Terr. Phys*., accepted for publication, 2012b.

Tsunoda, R.T., S.V. Thampi, T.T. Nguyen, and M. Yamamoto, On validating the relationship of ionogram signatures to large-scale wave structure, *J. Atmos. Solar-Terr. Phys*., accepted for publication, 2012.

Tulasi Ram, S., M. Yamamoto, R.T. Tsunoda, and S.V. Thampi, On the application of differential phase measurements to study the zonal large scale wave structure (LSWS) in the ionospheric electron content, *Radio Sci*., *47*, RS2001, doi:10.1029/2011RS004870, 2012.

3.3 LSWS CHARACTERISTICS FROM TEC MEASUREMENTS

We have shown for the first time that LSWS characteristics can be extracted from TEC measurements using radio beacons on board an equatorial-orbiting satellite [*Thampi et al*., 2009; *Tsunoda et al*., 2010; *Tulasi Ram et al*., 2012]. Before C/NOFS TEC measurements, only beacons on polar-orbiting satellites had been used to obtain information about plasma structure as a function of latitude. Figure 2 presents an example of our results [from *Tulasi Ram et al*., 2012]. The cluster of three receiving stations for these measurements was located in Vietnam. The LSWS can be clearly seen in panel (c). Peak-to-peak amplitudes as small as 0.2 TEC units

are easily detectable; zonal wavelengths in this example range from 275 to 615 km, typical of those associated with LSWS. The alignment in longitude of peaks and valleys found in the three curves is strong evidence that LSWS is aligned with geomagnetic field lines (because the magnetic declination over Vietnam is small). Radio wave scintillations in panel (d) are patchy and aligned with the west walls of the depleted regions. This finding is consistent with the development of plasma structure along the west wall of an upwelling in the bottomside *F* layer, as shown with ALTAIR measurements [*Tsunoda*, 1983]. These findings leave little doubt that the properties of LSWS deduced from C/NOFS TEC measurements are consistent with those deduced from ALTAIR.

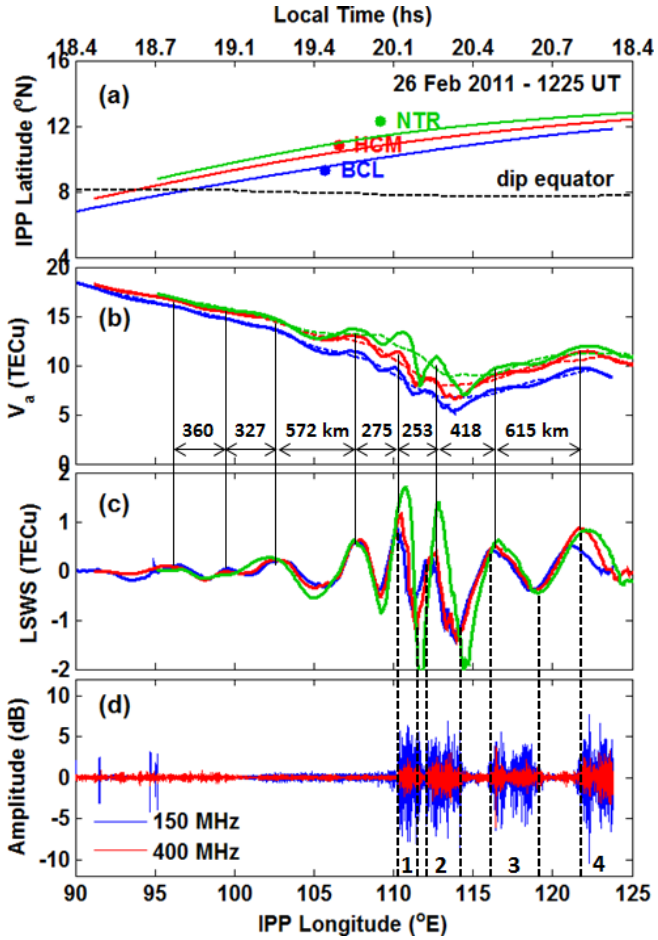

Figure 2. Results from a cluster of receivers at Bac Lieu (BCL), Ho Chi Minh City (HCM), and Nha Trang (NTR), in the Vietnam sector (from *Tulasi Ram et al*. [2011]). (a) Satellite tracks at the ionospheric penetration points (IPP) from each of the three stations. (b) Absolute TEC as a function of IPP longitude for BCL (blue), HCM (red), and NTR (green). (c) The residual perturbation in absolute TEC, which is interpreted as LSWS. Alignment in geographic longitude is equivalent to alignment with the geomagnetic field. (d) Amplitude scintillations at 150 and 400 MHz. The alignment of scintillation patches with the west walls of TEC depletions (upwellings) is associated with the LSWS.

3.4 PAUCITY OF LSWS DATA

We demonstrated conclusively that LSWS is essentially a spatial structure, which is zonally stationary during its growth phase. This important property of LSWS, first illustrated with ALTAIR measurements in a case study [*Tsunoda and White*, 1981], is the reason why LSWS has not been detected with other conventional sensors in use today (see discussion in *Tsunoda* [2005]). The paucity of LSWS data, until now, stems directly from using the wrong kinds of instruments to study ESF seeding. Indeed, LSWS has now been detected and described with TEC measurements using the radio beacons on the C/NOFS satellite [e.g., *Thampi et al*., 2009; *Tsunoda et al*., 2010, 2011; *Tulasi Ram et al*., 2012], as zonally varying spatial structures. Moreover, we have shown that LSWS is more or less stationary by comparing the TEC pattern found in successive passes of C/NOFS [*Tsunoda et al*., 2012], and we have shown that this behavior is exactly as expected from our understanding of equatorial electrodynamics.

To illustrate, we present a model result of the evening vortex [*Eccles et al*., 1999] in Figure 3, with yellow arrows drawn to indicate the drift velocity that should be associated with LSWS in the bottomside *F* layer. We can see that the zonal component of drift is weakly westward prior to 1800 LT, becomes zero near the beginning of the PSSR, then turns eastward for the remainder of the night. In other words, not surprisingly, the zonal flow of the bulk plasma in the bottomside *F* layer is essentially nonexistent during the PSSR. This flow pattern is completely consistent with observations [*Tsunoda et al*., 2012].

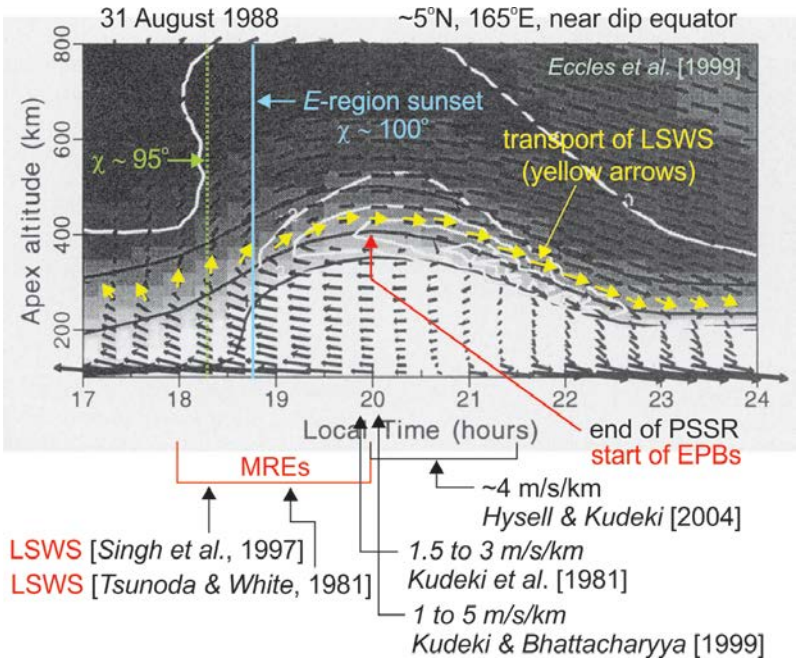

Figure 3. Model results of the evening vortex, from *Eccles et al*. [1999], with superimposed yellow arrows to show the flow direction along the bottomside *F* layer, where LSWS is situated.

3.5 FIRST APPEARANCE OF LSWS

We have shown with C/NOFS TEC data that LSWS can appear as early as the late afternoon, prior to ground sunset [*Thampi et al*., 2009; *Tsunoda et al*., 2010, 2011]. We can see from Figure 3 that LSWS appearance, with the solar zenith angle of about 87°, is not associated with

any velocity shear that may appear as part of the evening vortex. This finding is crucial because we can now conclude that LSWS is not produced by the collisional-shear instability [*Hysell and Kudeki*, 2004]. When this process was first proposed, it was considered the prime candidate for the seeding of EPBs. At that time, an attractive property of this process was its ability to select a preferred zonal wavelength, based on the strength of the velocity shear. The early appearance of LSWS also suggests the likelihood of some electrical loading by the solar-produced *E* layer, which must be considered. A concern is whether *E*-region dynamo and polarization effects might play a role in the initial appearance of LSWS.

3.6 MULTI-REFLECTED ECHOES: A MEANS FOR MONITORING LSWS PRESENCE

Given that C/NOFS passes occur only once every 90 minutes, we needed to find a more time-continuous method to monitor LSWS presence. Other than scanning radars (e.g., ALTAIR), the only instrument capable of providing information about spatial ionospheric structure (without horizontal transport) is an ionosonde [*Tsunoda*, 2005]. Toward this end, we have shown that multi-reflected echoes (MREs) are ionogram signatures for LSWS [*Tsunoda*, 2009; *Nguyen et al*., 2012; *Thampi et al*., 2012].

Figure 4 presents an example of MREs in an ionogram taken at Kwajalein. This signature is nothing more than multi-hop *F*-layer traces that have become aliased in ionograms because the selected inter-pulse period was set to a value less than the group delays of these multi-hop echoes. (The value of *n* indicates the number of hops associated with the labeled MRE.) The finding that the occurrence of MREs is only occasional has been used to infer that a certain amount of signal enhancement, through focusing, must be responsible. And, because focusing is likely produced by reflections from concave isodensity contours, we have concluded that MREs must appear when upwellings associated with LSWS are present. A new model has been derived to clarify our interpretation of how MREs are generated by shapes found in isodensity contours in the bottomside *F* layer [*Tsunoda*, 2012a].

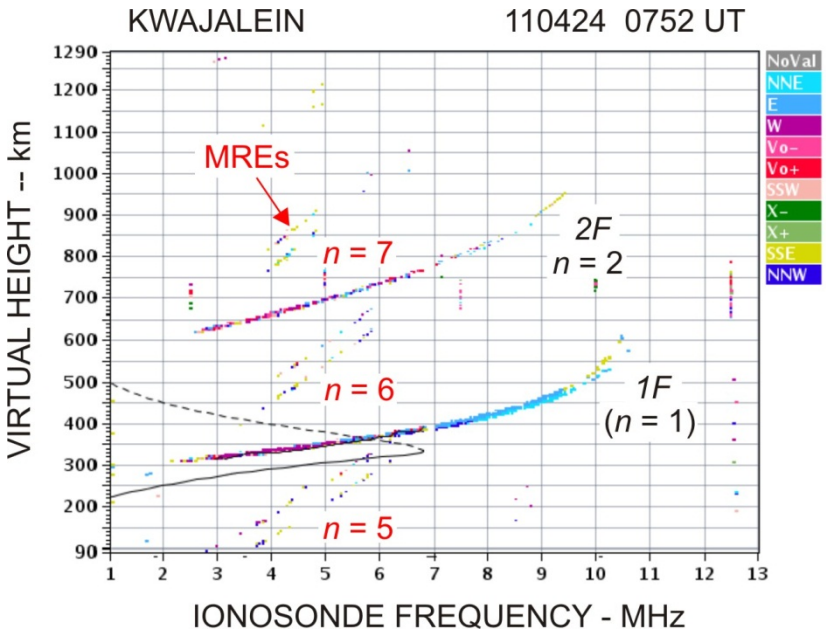

Figure 4. MREs in an ionogram taken at Kwajalein on 24 April 2004 [*Tsunoda et al*., 2012].

3.7 AMPLIFICATION OF LSWS DURING PSSR

Using MREs, we have found that their preferred time of occurrence is around *E*-region sunset [*Tsunoda*, 2009; *Tsunoda et al*., 2012]. To illustrate, Figure 5 presents the distribution of MRE occurrences as a function of local time. Analysis of a pair of C/NOFS passes, which straddled the PSSR, further substantiated this conclusion. We found that LSWS amplitude had indeed grown during the PSSR [*Tsunoda et al*., 2011]. Moreover, LSWS perturbations, which appeared well before *E*-region sunset, did not grow in amplitude until the PSSR. These results are consistent with the earlier finding that LSWS is zonally stationary during its growth phase, which occurs during the PSSR.

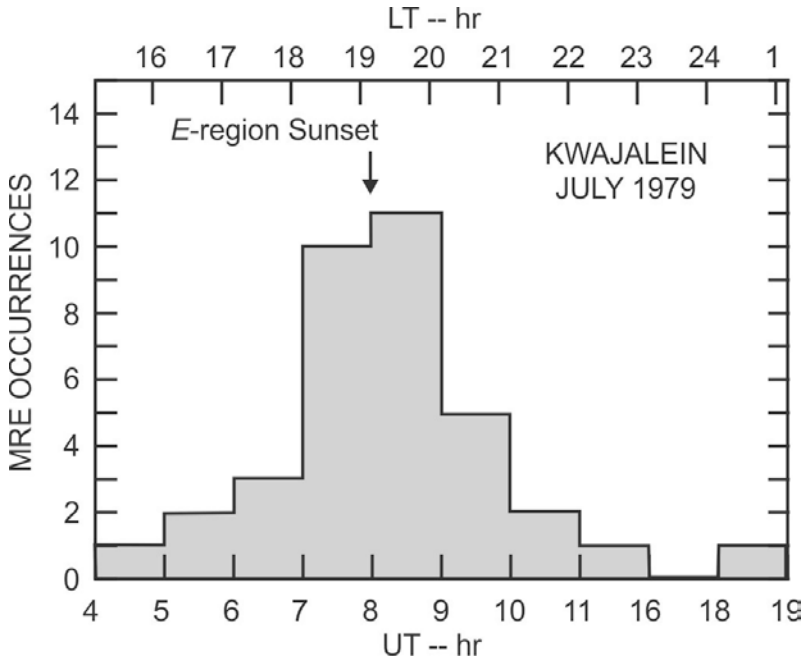

Figure 5. Histogram of MRE occurrences as a function of LT, obtained from ionograms taken at Kwajalein during two weeks in July 1979 [from *Tsunoda*, 2009]. The maximum, centered on *E*-region sunset, is consistent with the hypothesis that LSWS grows during the PSSR.

3.8 NEUTRAL-ION COUPLING

In our view, much can be learned by working backward from EPBs to LSWS, and from LSWS to its source. At present, the most likely source of LSWS is an atmospheric gravity wave (AGW) that is excited in the troposphere. Once excited, an AGW must propagate up into the thermosphere, where it interacts with the plasma in the bottomside of the equatorial *F* layer. Alternatively, the AGW could propagate up to the lower thermosphere, where it could also interact with the *E*-region plasma. Any perturbation electric field that might result from a polarization effect could then map up to the *F* region and become the source of LSWS. Given our finding that LSWS can appear in the late afternoon, when *E*-region effects may still be important, this possibility should not be ignored, but it has remained outside the scope of this project to become a topic for a future study. The question for this study was: how are the neutral-wind perturbations associated with an AGW communicated to the plasma? The next task, then, was to address the issue of neutral-ion coupling.

We considered two possible avenues for addressing neutral-ion coupling: one through the transverse transport (TT) of plasma, and the other through parallel transport (PT) [*Tsunoda*, 2012b]. The theoretical basis for neutral-ion coupling via TT was first proposed by Klostermeyer [1978]. Treating the simplest case, Klostermeyer assumed a zonally propagating plane AGW with vertically aligned phase fronts. Variations in the vertical wind produce a zonally directed Pedersen current, which is not divergence-free. Consequently, a zonally directed polarization electric field develops to cancel this current. This electric field, in turn, moves the plasma in the direction of the wind perturbation. Hence, source regions for zonally propagating AGWs would seem likely to be responsible for the appearance of LSWS. Given that most AGWs in the equatorial region are produced by convectively active regions within the inter-tropical convergence zone (ITCZ), it appeared that the latitudinal migration of the ITCZ with season could be used to test the hypothesis that AGWs are linked to LSWS. Two studies compared the global climatology of ESF [*McClure et al*., 1998] with the location of the ITCZ [*Tsunoda*, 2010a, c]. Both studies confirmed that ESF activity during the solstice displays a significant increase, when the ITCZ crosses the magnetic dip equator.

The proximity of the ITCZ to the dip equator did not, however, rule out the possibility that an AGW that is not propagating zonally could not produce a seed plasma perturbation. In fact, there seemed to be evidence that a traveling ionospheric disturbance (TID) could induce ESF activity and EPBs [e.g., *Abdu et al*., 2009]. This possibility raised the question of whether PT could be responsible for seeding. We performed an analysis to show that the perturbation responsible for seeding the plasma must be in the field-line-integrated Pedersen conductivity, not just the local plasma density. With this as a basis, we further showed that TT, not PT, is responsible for the neutral-ion coupling that must take place to produce a plasma seed.

We further tightened the requirement for neutral-ion coupling by showing that the AGW source region must be located on the dip equator to produce a plasma seed [*Tsunoda*, 2010c]. This is because AGW phase fronts are always tilted (not vertical). The only location where a polarization electric field can avoid electrical shorting (produced by the movement of electrons along geomagnetic field lines between adjacent phase fronts) is at the dip equator where the field lines are horizontal. We added further realism by assuming that AGW phase fronts are circular, and not planar [*Tsunoda*, 2010b]. Circular phase fronts are expected because each convectively active region, from which an AGW emanates, is usually geographically confined and resembles a point source. In contrast, planar phase fronts are expected from a convectively active region that is highly elongated, resembling a line source.

3.9 IDENTIFICATION OF SOURCE REGIONS FOR PARTICIPATING AGWS

These findings are quite important because we have uncovered a method by which we may be able to greatly simplify the forecasting of EPB activity on a day-to-day basis. To discuss this possibility, we note that highly convective regions, which are responsible for generating AGWs, can be identified from maps of cloud cover [e.g., *Tsunoda*, 2010a] or of outgoing longwave radiation (OLR) [e.g., *Tsunoda*, 2010c]. The problem of identifying source regions appeared to be overwhelming because clouds or active OLR regions are almost always present. It should be evident that the problem is greatly simplified by the requirement that the source region be located on the dip equator.

To illustrate, Figure 6 presents a sequence of satellite OLR maps, which were taken over Peru on 19-20 August 2012. The blue regions are associated with low OLR emission, which indicates the

high convective activity likely to generate AGWs. The band of speckled blue regions is associated with the ITCZ, which is located north of the geographic equator during northern summer months. The white curved line indicates the location of the magnetic dip equator. In this example, we were interested in whether ESF activity would develop over Jicamarca, which is marked by the white ellipse and labeled JRO. The PSSR occurred around 2300 UT, and a mesoscale convective complex (MCC) was located along the dip equator and to the east of JRO. Hence, the conditions for seeding appear to be ideal. Notice, however, that if all MCCs could generate AGWs that could participate in the seeding, we would have to consider all of the other blue regions that are embedded within the ITCZ. We have other examples in which an MCC is not located along the dip equator, but in most cases, MCCs within the ITCZ are always present. (In fact, ESF activity developed on this night.) Hence, we are now in position to properly test the hypothesis that an MCC must appear along the dip equator for ESF to develop that night. The validation of this hypothesis would provide a way to forecast the likely absence of ESF activity that night, if an MCC is not present. The finding that the MCC persisted for five hours is appealing because it leaves open the possibility that the lead time for forecasting could be several hours, or more.

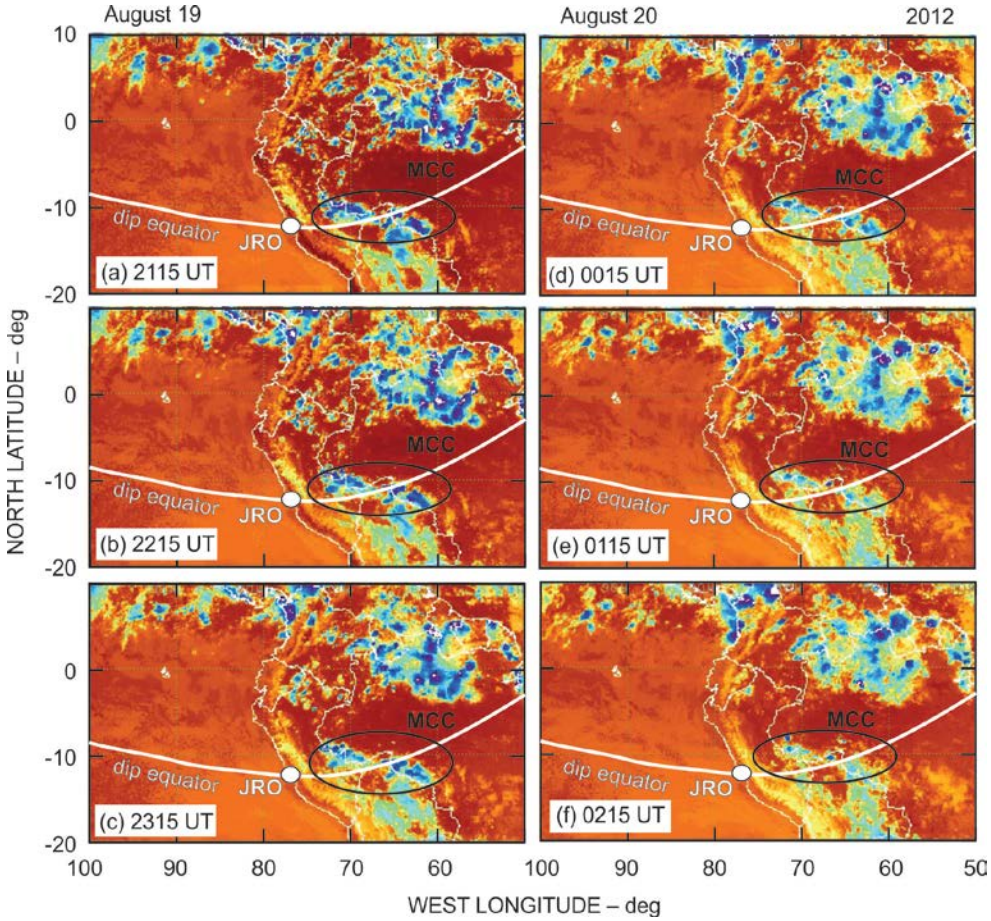

Figure 6. Satellite maps of MCC located to the east of Jicamarca (JRO), on 19-20 August 2012.

4 SUMMARY AND DISCUSSION

We can summarize the current status of understanding of EPB development with the set of sketches presented in Figure 7. In sketch (a), the blue dashed line represents the bottomside of the equatorial *F* layer; the upward slope depicts the PSSR; and the downward slope depicts the descent of the *F* layer after the PSSR. For these quiet, no-seed conditions, we expect an absence of MCC (in OLR maps) along the dip equator; an absence of LSWS along the bottomside *F* layer; and an absence of EPB development.

In the remaining three panels, we sketched the behavior, which we believe would follow the appearance of a seed perturbation. By seed (panel b – stage 1), we mean the presence of an MCC along the dip equator, which launches a zonally propagating AGW and leads to the appearance of LSWS, perhaps in the late afternoon. Assuming that the PSSR is significant, we envision amplification of LSWS during the PSSR (panel c – stage 2). During LSWS growth, we expect the appearance of MREs (Figures 4 and 5) and the development of plasma structure (but not EPBs) along the west wall of upwellings (Figure 2). Upwelling amplitude will be largest at the end of the PSSR, and we envision the first appearance of a primary EPB. By primary, we mean an EPB that grows from the crest of an upwelling (panel c – stage 2). After the end of the PSSR, we envision growth and bifurcation to occur in primary EPBs, and expect the appearance of secondary EPBs along the west walls of upwellings (panel d – stage 3).

The prospects for developing a space-weather forecasting capability are much more promising now than they were three years ago. For the first time, we are in position to flag the appearance of seed sources from available satellite maps of OLR. Establishing the chain of events from seed to LSWS to EPBs could produce a viable method for short-term forecasting, but much more research is required to establish these links. We must establish the reliability of MREs for detecting LSWS presence by comparing these ionogram signatures with LSWS in our TEC database. We still do not know the mechanism by which LSWS is amplified during the PSSR; this behavior is puzzling because LSWS grows in a region and at a time when EPBs do not. Understanding this source mechanism remains one of the key objectives of any future study, and we must emphasize that the LSWS database and a time-continuous means for monitoring LSWS presence (e.g., MREs) are pivotal to any ongoing research.

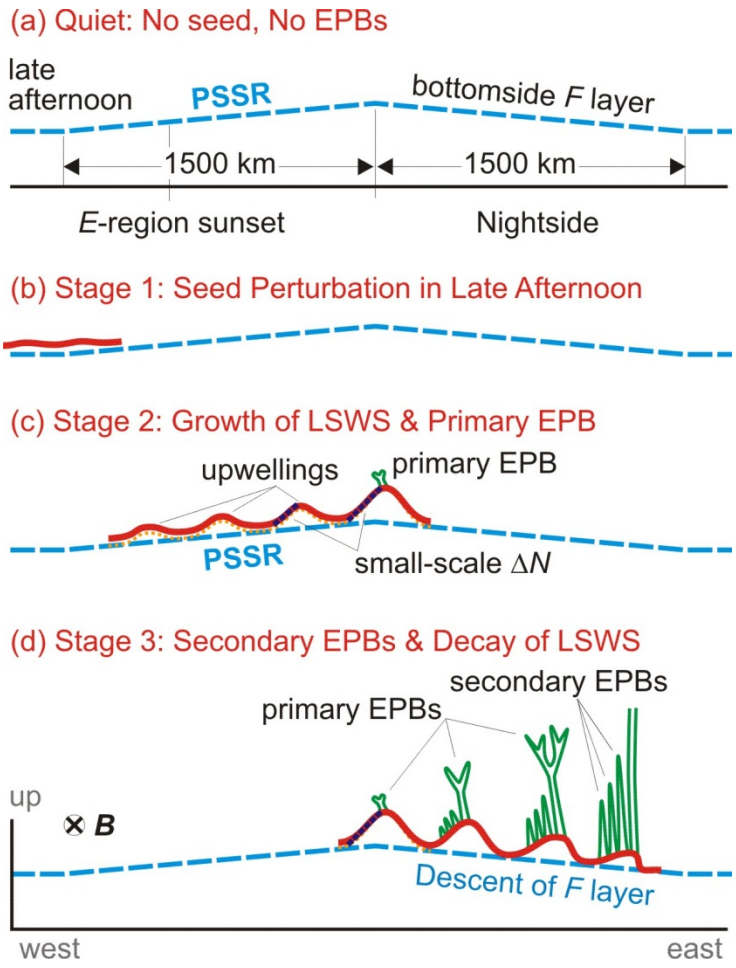

Figure 7. The working hypothesis for EPB development.

REFERENCES

Abdu, M.A., E. Alam Kherani, I.S. Batista, E.R. de Paula, D.C. Fritts, and J.H.A. Sobral, Gravity wave initiation of equatorial spread *F*/plasma bubble irregularities based on observational data from the SpreadFEx campaign, *Ann. Geophys.*, *27*, 2607, 2009.

Bernhardt, P.A. and C.L. Siefring, New satellite-based systems for ionospheric tomography and scintillation region imaging, *Radio Sci*., *41*, RS5S23, doi:10.1029/2005RS003360, 2006.

de La Beaujardiere, O., The C/NOFS Science Definition Team, *J. Atmos. Solar-Terr. Phys., 66*, 1573, 2004.

Eccles, J.V., N. Maynard, and G. Wilson, Study of the evening plasma drift vortex in the low-latitude ionosphere using San Marco electric field measurements, *J. Geophys. Res., 104*, 28,133, 1999.

Hysell, D.L. and E. Kudeki, Collisional shear instability in the equatorial *F* region ionosphere, *J. Geophys. Res.*, *109*, A11301, doi:10.1029/2004JA010636, 2004.

Klostermeyer, J., Nonlinear investigation of the spatial resonance effect in the nighttime equatorial *F* region, *J. Geophys. Res., 83*, 3753, 1978.

Li, G., B. Ning, M.A. Abdu, W. Wan, and L. Hu, Precursor signatures and evolution of post-sunset equatorial spread *F* observed over Sanya, *J. Geophys. Res., 117*, A08321, doi:10.1029/2012JA017820, 2012.

McClure, J.P., S. Singh, D.K. Bamgboye, F.S. Johnson, and H. Kil, Occurrence of equatorial *F* region irregularities: Evidence for tropospheric seeding, *J. Geophys. Res., 103*, 29,119, 1998.

Narayanan, V.L., A. Taori, A.K. Patra, K. Emperumal, and S. Gurubaran, On the importance of wave-like structures in the occurrence of equatorial plasma bubbles: A case study, *J. Geophys. Res., 117*, A01306, doi:10.1029/2011JA017054, 2012.

Nguyen, T.T., R.T. Tsunoda, and M. Yamamoto, On the relationship of multi-reflected echoes to large-scale wave structure and equatorial spread *F*, presented at the International Symposium for Equatorial Aeronomy, Paracas, Peru, March 2012.

Scannapieco, A.J. and S.L. Ossakow, Nonlinear equatorial spread *F*, *Geophys. Res. Lett., 3*, 451, 1976.

Singh, S., F.S. Johnson, and R.A. Power, Gravity wave seeding of equatorial plasma bubbles, *J. Geophys. Res., 102*, 7399, 1997.

Thampi, S.V., M. Yamamoto, R.T. Tsunoda, Y. Otsuka, T. Tsugawa, J. Uemoto, and M. Ishii, First observations of large-scale wave structure and equatorial spread *F* using CERTO radio beacon on the C/NOFS satellite, *Geophys. Res. Lett*., *36*, L18111, doi:10.1029/2009GL039887, 2009.

Thampi, S.V., R. Tsunoda, L. Jose, and T.K. Pant, Ionogram signatures of large-scale wave structure and their relation to equatorial spread *F*, *J. Geophys. Res*., *117*, A08314, doi:10.1029/2012JA017592, 2012.

Tsunoda, R.T., Magnetic-field-aligned characteristics of plasma bubbles in the nighttime equatorial ionosphere, *J. Atmos. Terr. Phys.*, *42*, 743, 1980.

Tsunoda, R.T., On the generation and growth of equatorial backscatter plumes. 2. Structuring of the west walls of upwellings, *J. Geophys. Res., 88*, 4869, 1983.

Tsunoda, R.T., On the enigma of day-to-day variability in equatorial spread *F*, *Geophys. Res. Lett., 32*, L08103, doi:10.1029/2005GL022512, 2005.

Tsunoda, R.T., Satellite traces: An ionogram signature for large-scale wave structure and a precursor for equatorial spread *F*, *Geophys. Res. Lett*., 35, L20110, doi:10.1029/2008GL035706, 2008.

Tsunoda, R.T., Multi-reflected echoes: Another ionogram signature of large-scale wave structure, *Geophys. Res. Lett*., 36, L01102, doi:10.1029/2008GL036221, 2009.

Tsunoda, R.T., On seeding equatorial spread *F* during solstices, *Geophys. Res. Lett*., *37*, L05102, doi:10.1029/2010GL042576, 2010a.

Tsunoda, R.T., On seeding equatorial spread *F*: Circular gravity waves, *Geophys. Res. Lett*., 37, L10104, doi:10.1029/2010GL043422, 2010b.

Tsunoda, R.T., On equatorial spread *F*: Establishing a seeding hypothesis, *J. Geophys. Res*., *115*, A12303, doi:10.1029/2010JA015564, 2010c.

Tsunoda, R.T., A simple model to relate multi-reflected echoes and satellite traces to large-scale wave structure, *Geophys. Res. Lett*., in review, 2012a.

Tsunoda, R.T., On seeding equatorial spread *F*: Parallel or transverse transport? *J. Atmos. Solar-Terr. Phys*., in review, 2012b.

Tsunoda, R.T. and B.R. White, On the generation and growth of equatorial backscatter plumes—1. Wave structure in the bottomside *F* layer, *J. Geophys. Res., 86*, 3610, 1981.

Tsunoda, R.T., R.C. Livingston, J.P. McClure, and W.B. Hanson, Equatorial plasma bubbles: Vertically elongated wedges from the bottomside *F* layer, *J. Geophys. Res., 87*, 9171, 1982.

Tsunoda, R.T., M.J. Baron, J. Owen, and D.M. Towle, ALTAIR: An incoherent scatter radar for equatorial spread *F* studies, *Radio Sci., 14*, 1111, 1979.

Tsunoda, R.T., D.M. Bubenik, S.V. Thampi, and M. Yamamoto, On large-scale wave structure and equatorial spread *F* without a post-sunset rise of the *F* layer, *Geophys. Res. Lett*., *37*, L07105, doi:10.1029/2009GL042357, 2010.

Tsunoda, R.T., M. Yamamoto, T. Tsugawa, T.L. Hoang, S. Tulasi Ram, S.V. Thampi, H.D. Chau, and T. Nagatsuma, On seeding, large-scale wave structure, equatorial spread *F*, and scintillations over Vietnam, *Geophys. Res. Lett*., *38*, L20102, doi:10.1029/2011GL049173, 2011.

Tsunoda, R.T., S.V. Thampi, T.T. Nguyen, and M. Yamamoto, On validating the relationship of ionogram signatures to large-scale wave structure, *J. Atmos. Solar-Terr. Phys*., in review, 2012.

Tulasi Ram, S., M. Yamamoto, R.T. Tsunoda, and S.V. Thampi, On the application of differential phase measurements to study the zonal large scale wave structure (LSWS) in the ionospheric electron content, *Radio Sci*., *47*, RS2001, doi:10.1029/2011RS004870, 2012.